Analysis of the Structure and Durability of Refractory Castables Impregnated with Sodium Silicate Glass

Jurgita Malaiškienė *, Valentin Antonovič, Renata Boris, Andrius Kudžma, Rimvydas Stonys

Posted Date: 6 November 2023

doi: 10.20944/preprints202311.0367.v1

Keywords: refractory castable; impregnation; liquid sodium silicate glass; alkali resistance; physical and mechanical properties, thermal shock resistance

Article

Analysis of the Structure and Durability of Refractory Castables Impregnated with Sodium Silicate Glass

Jurgita Malaiškienė *, Valentin Antonovič, Renata Boris, Andrius Kudžma and Rimvydas Stonys

Institute of Building Materials, Laboratory of Composite Materials, Vilnius Gediminas Technical University, Vilnius, Lithuania

* Correspondence: jurgita.malaiskiene@vilniustech.lt; Tel.: +370-5-2512329

Abstract: This study examines the impact of the impregnation of fireclay-based conventional (CC) and medium cement castables (MCC) with liquid sodium silicate glass under vacuum conditions. The goal is to assess how this treatment affects physical, mechanical properties, and durability (alkali and thermal shock resistance) of these castables used in biomass combustion boilers, where they are exposed to temperatures up to 1100°C. The research work employs standard test methods to evaluate physical and mechanical properties. Additionally, advanced techniques such as scanning electron microscopy (SEM), energy-dispersive X-ray spectroscopy (EDS), X-ray diffraction (XRD), and specific tests for alkali resistance and thermal shock resistance are used. The research findings suggest that impregnation with sodium silicate glass under vacuum significantly enhances the alkali resistance of both CC and MCC castables. This improvement is primarily due to the reduction in porosity and the increase in density. SEM images reveal that impregnated samples are coated with a glassy layer and the pores are partially filled with sodium silicate. Tests for alkali resistance demonstrate the formation of a protective glassy layer (with a thickness of 0.9-1.5 mm) on the castable surfaces, thereby reducing further penetration of alkali into deeper layers of the samples. However, it is important to mention that impregnated refractory castables have reduced resistance to thermal shock cycles.

Keywords: refractory castable; impregnation; liquid sodium silicate glass; alkali resistance; physical and mechanical properties; thermal shock resistance

1. Introduction

In recent decades, there has been a widespread adoption of biomass combustion boilers used as a cost-effective option for energy production [1,2]. These boilers utilize renewable energy sources such as wood, straw, mixed municipal waste, and other materials to reduce the reliance on fossil fuels in order to align with ambitious targets set by the European Union aiming for at least 27% renewable energy by 2030 [3]. The lining of these biomass boilers is constructed using various refractory materials, including castables, which are carefully selected for their ability to withstand high temperatures and to maintain structural integrity over extended periods [4,5]. For instance, in the demanding conditions of some species of biomass combustion where temperatures can range up to 1200°C, it is advised to opt for chemically resistant refractory castables containing SiC, or alumina-chrome, engineered to withstand extreme operating conditions [4].

However, wood biofuel boilers predominantly operate at temperatures below 1100°C, making them prime candidates for castables enriched with aluminosilicate aggregates like fireclay or mullite [5]. Regrettably, these castables exhibit limited resistance to alkali corrosion, which often leads to premature degradation attributed to the corrosive influence of alkalis present in the refractory materials and fuel [6]. The genesis of alkali corrosion lies in the formation of potassium/sodium oxides and their corresponding salts, a consequence of biomass combustion. The alkaline content of the resultant ash is influenced by a myriad of factors, including wood type, grade, and quality [7]. Furthermore, the using of alkaline salts, despite preventing wood fuel freezing in winter conditions, significantly amplifies the concentration of alkaline compounds (sodium and potassium), thereby

 doi:10.20944/preprints202311.0367.v1

lowering the melting point of the ash and potentially causing it to fall below the boiler's operational temperature [8].

The intricate reactions responsible for reducing the ash/slag melting point are rooted in the interaction between potassium and carbon in various forms, culminating in the formation of alkaline compounds [9]. Corrosion, in this context, ensues from the dissolution of the refractory material and its intricate interplay with the alkaline molten phase. Additionally, it can manifest as reactions with alkaline vapors, the presence of alkaline compounds in liquid or solid-state, and the infiltration of alkaline vapors or the molten phase into the material's porous structure, thereby giving rise to altered zones within the material matrix [10]. These alkali reaction byproducts, including leucite ($KAlSi_2O_6$) and kalsilite ($KAlSiO_4$), demonstrate a peculiar characteristic by occupying volumes greater than that of the original material. This phenomenon is commonly referred to as "alkali bursting" [11–13]. Importantly, the extent of alkali reaction damage is linked to the porosity of the material [14], with materials of lower porosity and superior gas impermeability displaying greater resistance to such forms of damage [15,16].

A prevalent choice for binders in refractory castables is calcium aluminate cement [17]. In comparison to conventional castables, low cement and ultra-low cement castables have surged in popularity, thanks to their lower porosity, higher mechanical strength within critical temperature ranges, impressive erosion resistance, and elevated refractoriness [18–20]. These castables incorporate various ultra-dispersive additives, such as silica fume and calcined alumina, alongside deflocculants that effectively diminish cement content to a mere fraction compared to conventional refractory castables [21]. However, it is important to note that these low and ultra-low cement castables often prove sensitive to factors such as ambient conditions, water content, mixing parameters, and more, making the production process challenging [22–24].

Meanwhile, medium cement castables have gained recognition for their capacity to maintain consistent quality even under varying manufacturing conditions, setting them apart as a favorable choice for biofuel boiler installations [22,23]. While lower porosity of castables can undoubtedly enhance their durability within alkaline environments, it is important to acknowledge that over time alkali may still infiltrate the castable structure and engage with aluminosilicate aggregates [21]. One promising avenue for mitigating alkali-induced damage involves the addition of ground quartz sand to fireclay refractory castables, a practice known to stimulate the formation of a protective glassy layer on the castable surface when subjected to alkali salts at elevated temperatures [24,25]. However, it is imperative to exercise caution when determining the quantity of the quartz sand added due to the polymorphic transformations of SiO_2 that transpire at specific temperature thresholds [26].

Impregnation of the material could be also an effective method to substantially decrease the porosity of refractory castables and increase their alkali resistance. In the field of impregnation technology, suspensions of various materials are employed [22,23], and the specific materials used for impregnation can vary in their roles. Authors reported [27] a significant enhancement in corrosion resistance of a chromium-magnesium material after impregnation with suspensions containing nano-Cr_2O_3 and nano-Fe_2O_3 particles. The nanoparticles within the material pores dissolved when exposed to the slag melt, resulting in an increase in its viscosity and a reduction in the ability of the slag melt to penetrate. Research on the resistance of refractory concrete to alkali attack at 1100°C temperature revealed that incorporating 2.5% milled quartz sand and impregnating the samples with a SiO_2 sol can lead to the formation of a protective glassy barrier. This barrier effectively blocks further penetration of potassium and prevents additional cracking and disintegration of refractory concrete [21].

A cheaper material, such as liquid sodium silicate glass, could be also used as an impregnant for fireclay refractory castables [28]. Liquid sodium silicate glass, when employed as a binder in refractory castables, serves as a flux when subjected to high temperatures and reduces the required operating temperature for aluminosilicate refractory castables by approximately 200–300°C. Research findings, however, indicate that refractory castables containing a sodium silicate liquid glass binder can achieve operating temperatures of 1100 –1300°C [28]. This means that the permitted use

Preprints (www.preprints.org) | NOT PEER-REVIEWED | Posted: 6 November 2023 doi:10.20944/preprints202311.0367.v1

temperatures of such materials fully satisfy the conditions in which wood biofuel boilers are operated.

The purpose of this study was to assess how the properties (density, cold crushing strength, porosity, microstructure, as well as alkali and thermal shock resistance) of fireclay refractory castables change when they are impregnated with liquid sodium silicate glass under vacuum.

2. Materials and Methods

Calcium aluminate cement produced by Górka Cement Company (G70; Poland) and Istra-40 (ISTR) produced by Calucem GmbH (Germany) were used as binders for refractory castable. The chemical composition of cement is presented in Table 1. G70 has the Blaine specific surface area of 450 m^2/kg and ISTR has 295 m^2/kg. Reactive alumina CTC 20 (RA; Almatis Germany) containing 99.7% Al_2O_3 with Blaine fineness of 2100 m^2/kg and calcined alumina CT 19 (CA) containing 99.8% Al_2O_3 with Blaine fineness of 400 m^2/kg were additionally used for the preparation of medium cement castables. In conventional (CC) and medium cement (MCC) castables, microsilica, containing 96% SiO_2 (MS, RW-Fuller; RW Silicon GmbH, Germany) with an average diameter approximately 150 nm, was used. Fireclays FA35 and FA45 from Tabex-Ozmo (Poland) were used as aggregates (<4mm). Additionally, the same fireclay after 1 h milling and sieving through a sieve with a mesh size of 0.14mm was used as fine aggregate. The refractoriness values of FA35 and FA45 were 1710°C and 1750°C, respectively. The chemical composition of both fireclay aggregates is presented in Table 1. Milled quartz sand (MQS) from AB Anykščių kvarcas (Lithuania) containing 99.2% SiO_2, with Blaine fineness of 490 m^2/kg was used for the improvement of fireclay refractories resistance to alkali attack [29]. The following deflocculants were used: Castament FS20 and FS30 from BASF Construction Solutions GmbH (Germany) and technical sodium tripolyphosphate NT. Liquid sodium silicate glass with a SiO_2/Na_2O molar ratio of 3.3 and a density of 1.33g/cm^3 was used for the impregnation of the samples. Drinking water was used to prepare the mixtures. The chemical reagent K_2CO_3 (99.0%, Sigma Aldrich, USA) was used for the testing of alkali resistance.

Table 1. Chemical compositions of G70, ISTR, FA35 and FA45.

Oxide	G70	ISTR	FA35	FA45
Al_2O_3	71.0	40.8	36.6	44.3
CaO	28.5	38.5	3.1	0.6
SiO_2	0.3	4.5	53.7	49.5
Fe_2O_3	0.2	15.0	3.3	2.1
MgO	–	1.2	0.7	0.9
K_2O	–	–	1.0	0.7
TiO_2	–	–	1.3	1.4

Samples in size 70×70×70mm and 160×40×40mm (for thermal shock resistance) were prepared from the raw materials listed above. The compositions of the samples are presented in Table 2.

Table 2. The compositions of refractory castables.

Composition,%	G70	ISTR	MS	FA35 <0.14 mm	FA45 <0.14 mm	FA35 <4 mm	FA45 <4 mm	RA	CA	MQS	Water
CC-1	-	25	2.5	10	-	60	-	-	-	2.5	11.3
CC-2	-	25	2.5	-	10	-	60	-	-	2.5	7.4
MCC-1	12	-	5	8	-	60.5	-	5	7	2.5	8.9
MCC-2	12	-	5	-	8	-	60.5	5	7	2.5	7.1

* For CC deflocculant FS30 0.1% was used, for MCC FS20 0.1% and NT 0.1% were used. Deflocculants and water were added up to 100%.

Preprints (www.preprints.org) | NOT PEER-REVIEWED | Posted: 6 November 2023 doi:10.20944/preprints202311.0367.v1

Dry components presented in Table 2 were mixed in a Hobart planetary mixer for 5 min and then mixed with water for 3 min. The samples were kept for 72h at 20±1°C, relative humidity about 50%, then dried at 110°C for 48h and fired at 1100°C for 5h. The preparation and treatment of the refractory concrete samples (curing, drying, and thermal treatment) were carried out according to the requirements of LST EN ISO 1927-5:2013. Some of the fired samples were subsequently impregnated with liquid sodium silicate glass under vacuum (1atm), dried, and fired in a similar manner.

Physical and mechanical characteristics (density, cold crushing strength) were determined according to LST EN ISO 1927-6:2013, three samples from each composition were used for the testing. Thermal shock resistance was determined by evaluating changes in ultrasonic pulse velocity [28], when the samples are cyclically heated at 1100°C and cooled between 2 metal plates filled with cold water. Before testing (Uo), the ultrasonic pulse velocity was measured after 3 (U3c) and 7 (U7c) cycles and the relative thermal shock resistance R was calculated according to the formula:

$$R = \frac{\sqrt{U3c \times U7c}}{Uo} \times 100\% \quad (1)$$

The propagation time of ultrasound waves was determined by using Pundit 7 instrument (converter frequency = 54 kHz) calculating the ultrasonic pulse velocity (UPV, m/s):

$$UPV = \frac{l}{\tau}. \quad (2)$$

where: l is the length of the specimen, m; s is signal propagation time, s.

The modulus of elasticity E was calculated from the equation 3:

$$E = U^2 \cdot \rho \frac{(1+\mu)(1-2\mu)}{1-\mu} \quad (3)$$

where: U is the UPV (m/s), ϱ is the density of concrete (kg/m^3), and μ is Poisson's coefficient, which is 0.17 for all types of concrete [30,31].

The crucible method (ASTM C 454–83:2007) was used to evaluate the resistance of refractory castables to alkali corrosion. Castable cubes of 70×70×70mm with a hole of diameter 20mm and height 30mm were produced (3 specimens per composition). The formed samples were cured in natural conditions for 72h, then dried at the temperature of 110±5°C for 48h and fired at 1100±5°C for 5h. A total 9g of K_2CO_3 was added to the hole, which was covered with a castable plate of the same composition, and the specimens were fired at the temperature of 1100±5°C for 5h. After repeated tests (9 g of K_2CO_3 were added for each test), the specimens were visually examined for microcracks. Some specimens were cut into two pieces along the cylindrical axis after 6 and 20 cycles, and the affected area of the castable was examined.

The chemical composition of the materials was determined using X-ray fluorescence spectrometer ZSX Primus IV (Rigaku, Japan) equipped with an Rh tube with an anode voltage of 4kV. Tablet-shaped samples with a diameter of 40mm were prepared and compressed at 200kN for analysis.

X-ray diffraction (XRD) analysis was performed using a DRON-7 diffractometer (Bourevestnik, Russia) with Cu Kα (λ = 0.1541837 nm) radiation. The following test parameter values were set: 30kV voltage, 12mA current, and 2θ diffraction angle ranging from 4° to 60° with increments of 0.02° measured every 2s. The existing phases were identified by comparing the XRD diffractograms with standard diffraction patterns provided by the International Centre for Diffraction Data (ICDD).

Microstructural analysis was performed using a JSM-7600F scanning electron microscope (JEOL, Japan). The analysis was performed at an accelerating voltage of 10kV in the secondary electron mode for image formation. Initially, the surface was covered with a layer of electrically conducting material using a QUORUM Q150R ES device (Quorum Technologies ltd., Germany). Some polished samples were used to evaluate the thickness and chemical composition of the potassium-treated surface layer. X-ray microanalysis was performed by the Energy Dispersion Spectrometer (EDS) Inca Energy 350 (Oxford Instruments, UK), using Silicon Drift type detector X-Max20. The INCA software package (Oxford Instruments, UK) was used. Three points per plane were tested, starting from the surface exposed to corrosion attack and going down every 100μm, with 3 more points selected in the next plane. In this way the elemental composition of the test sample was determined down to 3000μm. An area of corrosion free material at 10mm distance from the exposed surface was also tested.

 doi:10.20944/preprints202311.0367.v1

3. Results

3.1. The impact of impregnation on refractory castable chemical and mineral composition, and microstructure after firing at 1100°C

The chemical composition of the samples (Table 3) showed that, irrespective of the type of concrete, there is a five times higher sodium oxide content on the surface of the samples impregnated with sodium silicate solution. A higher silica content up to 13–69%, depending on the composition of concrete, was also observed.

Table 3. Chemical composition of control and impregnated castables.

Composition of castable	Chemical composition, mass %									
	Al_2O_3	SiO_2	CaO	Fe_2O_3	K_2O	Na_2O	MgO	ZrO_2	TiO_2	P_2O_5
Control samples										
CC-1	29.3	35.4	22.6	9.20	0.27	0.20	0.51	0.09	1.59	0.43
CC-2	29.2	32.1	25.5	10.3	0.30	0.12	0.55	0.04	1.24	0.14
MCC-1	51.1	36.2	8.36	1.27	1.14	0.55	0.30	0.03	0.40	0.24
MCC-2	52.8	34.6	8.15	1.10	0.64	0.46	0.40	0.02	0.77	0.73
Impregnated samples										
CC-1	15.3	40.0	33.1	7.42	0.22	0.91	1.34	0.11	1.00	0.28
CC-2	11.5	41.3	35.2	8.41	0.19	0.63	1.20	0.06	0.93	0.36
MCC-1	30.2	51.7	12.2	1.15	1.10	2.60	0.37	0.05	0.00	0.14
MCC-2	22.0	58.6	12.6	1.42	2.11	1.96	0.53	0.02	0.23	0.38

It was determined that after firing at 1100°C, sodium silicate influences the mineralogical composition of refractory castable. XRD analysis (Figure 1) showed that the same compounds identified in the control and impregnated samples (anorthite, gehlenite, mullite, tridymite, quartz, corundum, grossite), but the intensities of anorthite were much higher in impregnated samples. According to the literature, anorthite has good physical properties, such as low thermal expansion coefficient, good thermal shock resistance at high temperatures and thus it could improve the properties of refractory castables [32].

Preprints (www.preprints.org) | NOT PEER-REVIEWED | Posted: 6 November 2023 doi:10.20944/preprints202311.0367.v1

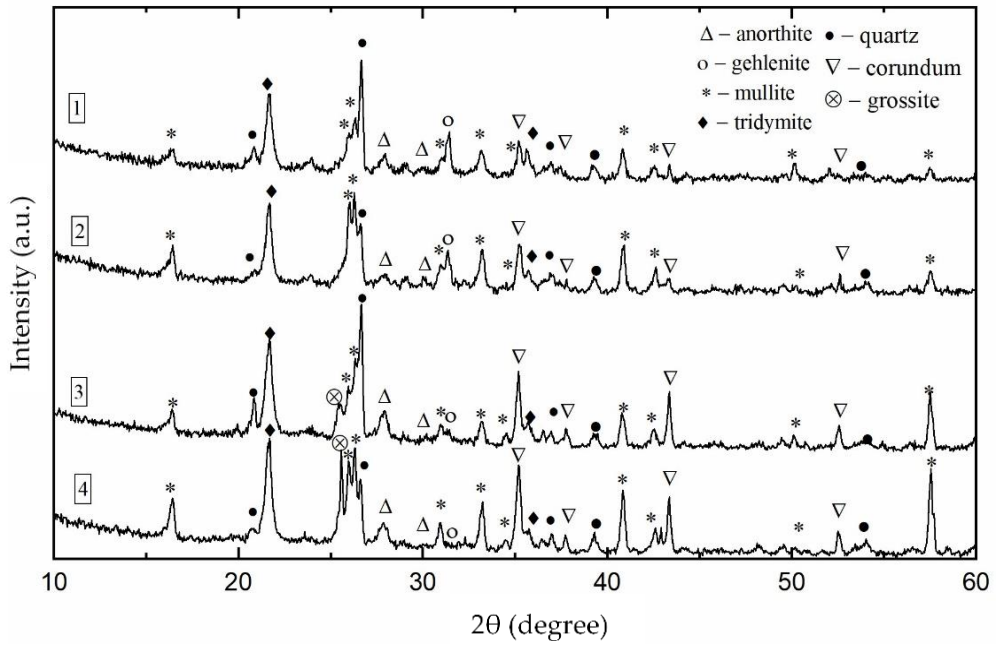

a)

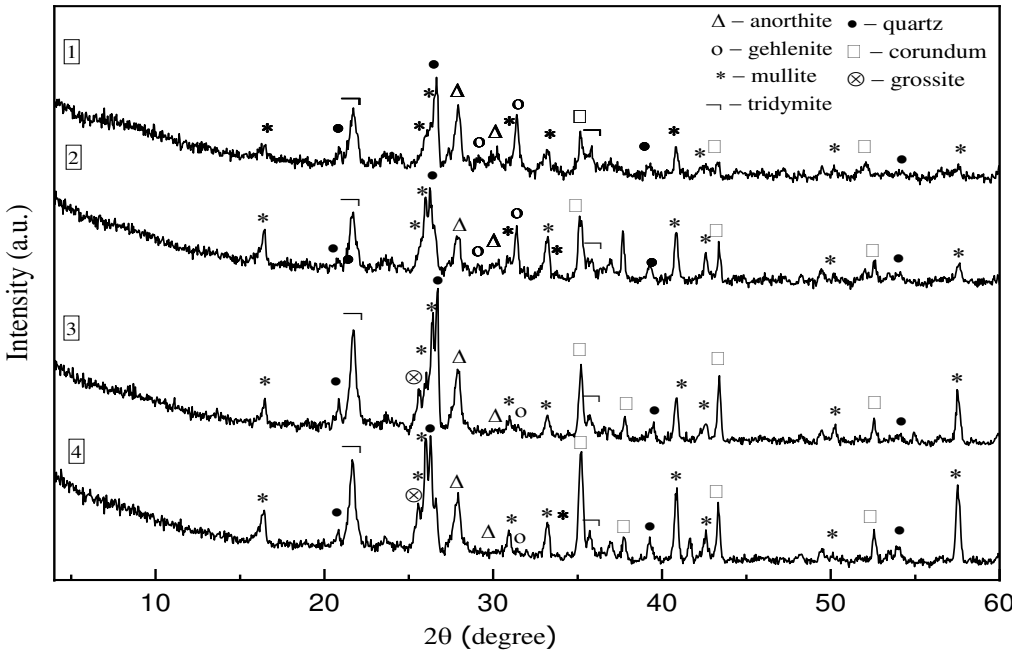

b)

Figure 1. Xray analysis of control (a) and impregnated (b) samples.

SEM images show that the microstructure of impregnated and fired at 1100°C samples, regardless of composition, is denser (Figure 2a-d) compared with control samples (Figure 2e-h). Porosity and the diameter of many pores reduced when the refractory castable was exposed to liquid glass under vacuum as the resulting sodium silicate partially filled the pores and capillaries. After firing, water from liquid glass evaporated forming hardened sodium silicate films that prevented the vaporization of residual moisture and could cause the bloating of sodium silicate mass. Sodium silicate at 300–500°C includes amorphous silica, the crystallization of which starts at 600°C and the crystalline phase vanishes completely at 900°C, and then porosity drops with vitrification [33].

Preprints (www.preprints.org) | NOT PEER-REVIEWED | Posted: 6 November 2023 doi:10.20944/preprints202311.0367.v1

Additionally, at 900°C and above sodium silicate starts reacting with other refractory raw materials and forms new compounds, or higher quantity of them, for example anorthite (Figure 1).

The most visible changes in the microstructure were observed in the impregnated samples MCC-2, where the blown sodium silicate zones in the pores are visible (Figure 2d).

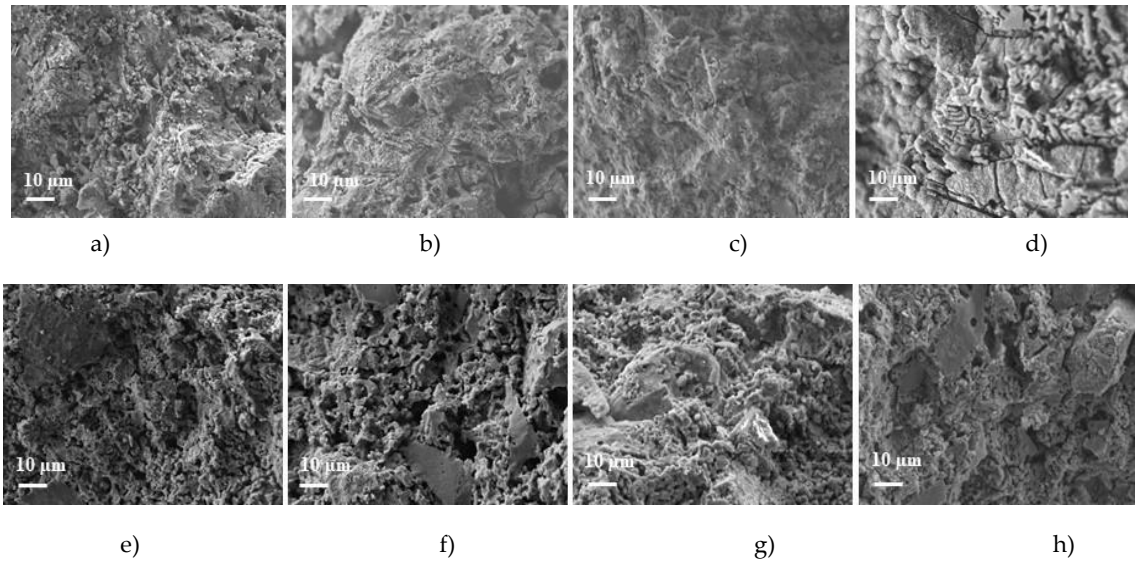

Figure 2. The images of control and impregnated samples: a) CC-1- impregnated, b) CC-2- impregnated, c) MCC-1- impregnated, d) MCC-2- impregnated, e) CC-1 control, f) CC-2 control, g) MCC-1 control, h) MCC-2 control.

3.2. The impact of impregnation on physical and mechanical properties of refractory castables after firing at 1100°C

Density and UPV values are shown in Figure 3. It is seen that both properties of castables improved after impregnation. Density did not increase significantly, only 0.5–1.9%, but UPV increased from 2.6% till 6.5% due to the formation of a denser structure and the filling of some pores with liquid silicate glass. A more significant improvement of these properties was observed in samples CC-1 and MCC-1, where a lower grade fireclay (FA35) was used, and this improvement can be related with a higher initial porosity of these samples compared to CC-2 and MCC-2 (Figure 4).

The cold crushing strength (Figure 5) of all types of refractory castables impregnated with liquid sodium silicate glass increased from approximately 10% to 18%. The increase in cold crushing strength of the impregnated samples resulted from the formation of a denser structure and a decrease in porosity (Figure 2, Figure 4).

Preprints (www.preprints.org) | NOT PEER-REVIEWED | Posted: 6 November 2023 doi:10.20944/preprints202311.0367.v1

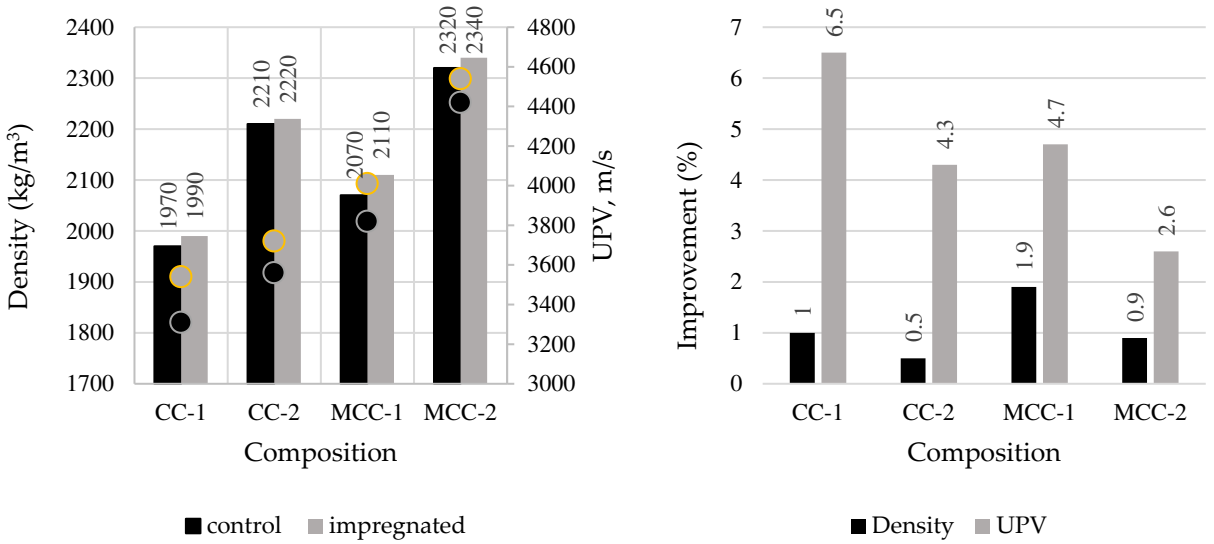

Figure 3. Results of density and UPV of control and impregnated samples.

After impregnation, it was found that the porosity (Figure 4) of all types of refractory castables decreased by approximately 10% because the pores were filled with sodium silicate glass. Similar results are reported in article [34], but the authors used silica sol for the impregnation of fireclay refractory castable. In that case the compressive strength increased approximately 40% because of SiO_2 sol filling the cracks and the presence of open pores in the samples and the increased amount of mullite at high temperatures through the reaction of ultrafine Al_2O_3 with nano-sized SiO_2 particles. In this work it was determined that cold crushing strength increases till 18%, but porosity decreases about 10% and the improvement in strength could have resulted from chemical reactions and the formation of higher quantities of some thermally stable compounds, such as anorthite (Figure 1).

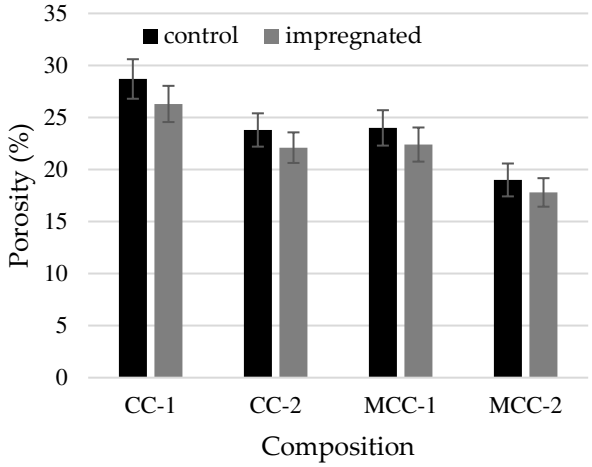

Figure 4. Porosity of control and impregnated samples.

Preprints (www.preprints.org) | NOT PEER-REVIEWED | Posted: 6 November 2023 doi:10.20944/preprints202311.0367.v1

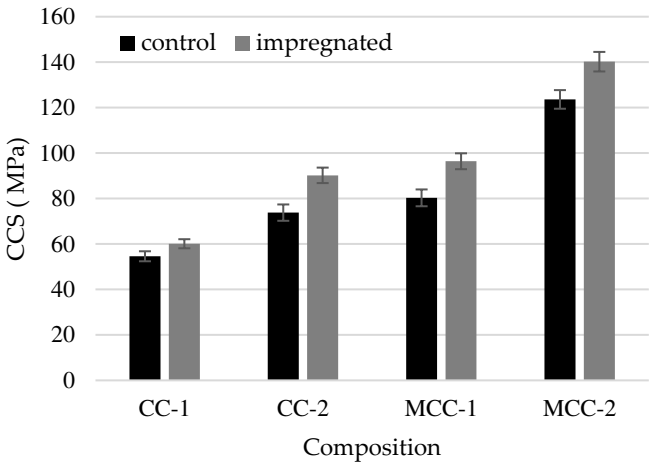

Figure 5. CCS of control and impregnated samples.

The diagram above (Figure 4) illustrates that the porosity of refractory castables varies significantly among different compositions, ranging from approximately 16% to around 29%. This difference in the compositions of the refractory castables was chosen to evaluate the effectiveness of impregnation for different refractory castables.

3.3. The impact of impregnation on alkali resistance at 1100°C

According to conclusions presented in the literature *[17–19]*, the densified microstructure of the surface should increase the alkali resistance of refractory castables with fireclay fillers at high temperatures. Figure 6 presents the images of cut control and impregnated refractory castable samples after 20 cycles of alkali exposure. A clearly visible white glassy barrier with a width of about 1-2mm was formed on the surface of impregnated sample holes into which the potassium carbonate was added. At high temperatures, sodium from impregnant and potassium from reagent reacted with refractory compounds and formed sodium alumina silicate and potassium alumina silicate layers. Then the viscosity of the formed glassy layer on the surface of the sample increased and alkali reagent (potassium) could not penetrate deeper into the material. Thus, the glassy layer acts as a protective barrier, making it difficult for the alkali to penetrate the material.According to the $Na_2O–Al_2O_3–SiO_2$ phase diagram [35], liquid sodium silicate can further react to form albite ($NaAlSi_3O_8$) and nepheline ($NaAlSiO_4$). Additionally, it was found [36] that Al_2O_3 can influence viscous glass melting temperature and its viscosity; therefore, the melting temperature and viscosity values of formed glass on the surface of the sample tend to increase [37].

Milled quartz additive participated in the building of the protective barrier in control samples as well, but after 20 alkali exposure cycles this barrier became weaker and the samples expanded, leading to expansion caused deformations at the top of the samples (Figure 6 a-d).

a) b) c) d)

Preprints (www.preprints.org) | NOT PEER-REVIEWED | Posted: 6 November 2023 doi:10.20944/preprints202311.0367.v1

e) f) g) h)

Figure 6. Images of impregnated refractory castable samples after 20 cycles of alkaline exposure: a) CC-1 control, b) CC-2 control, c) MCC-1 control, d) MCC-2 control, e) CC-1- impregnated, , f) CC-2- impregnated g) MCC-1- impregnated, h) MCC-2- impregnated.

A comparison of the depth of potassium penetration between control and impregnated samples after 6 alkali corrosion cycles showed (*Figure* 7) that impregnated samples had a significantly lower potassium content of about 40% in the surface layer and 30–80% at 10mm depth from the surface. Hence, sample impregnation significantly reduces potassium penetration into refractory castables and increases the resistance to alkali corrosion due to the formation of a more stable protective barrier.

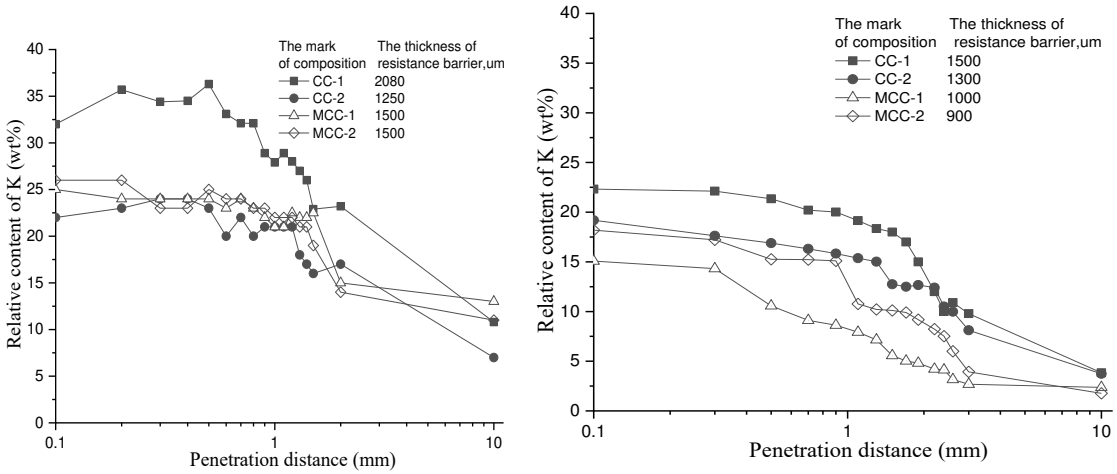

a) b)

Figure 7. Relative content of potassium at different penetration distances: a) control samples, b) impregnated samples.

3.4. The impact of impregnation on elasticity modulus and thermal shock resistance at 1100°C

After the impregnation, the modulus of elasticity of refractory castable (*Figure* 8) samples CC-1, CC-2, MCC-1, MCC-2 increased 16%, 10%, 13% and 7% respectively. Following the principles of thermoelastic theory concerning crack nucleation, engineers and researchers often employ the stress-to-elastic modulus ratio (σ/E) as a measure to evaluate the capacity of a material to withstand the initiation of cracks [33,38]. However, a material possessing a higher modulus of elasticity tends to exhibit diminished thermal shock resistance [21,34,39], as well as result of the work illustrated in Figure 9.

Thermal shock resistance (*Figure* 9) of impregnated samples compared to control samples decreased from approximately 8% (CC-2, MCC-2) to 12% (CC-1, MCC-1).

Preprints (www.preprints.org) | NOT PEER-REVIEWED | Posted: 6 November 2023 doi:10.20944/preprints202311.0367.v1

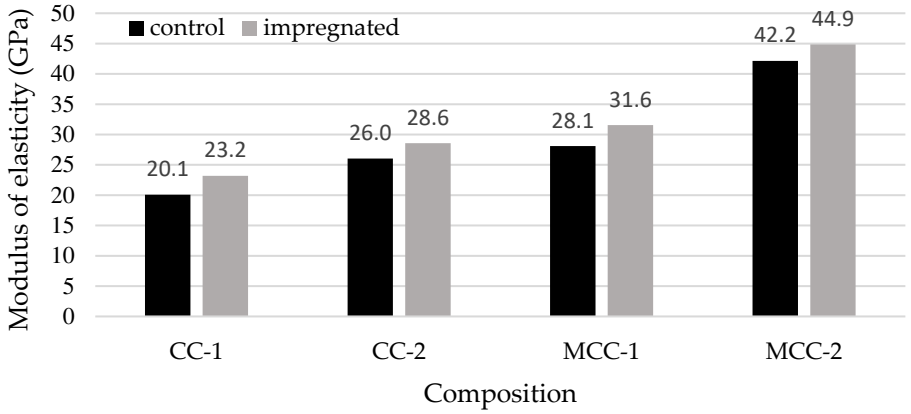

Figure 8. Modulus of elasticity of control and impregnated samples.

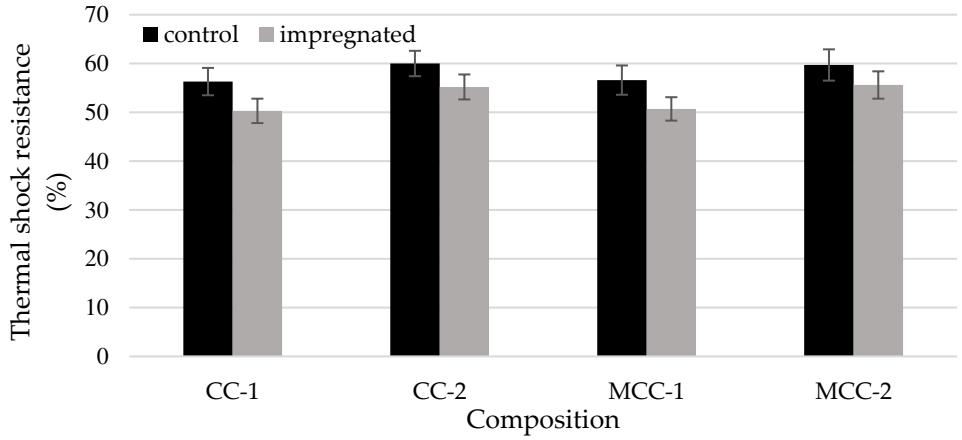

Figure 9. The comparison of thermal shock resistance of control and impregnated samples.

In this study, the impregnation technology was used for a more accurate laboratory testing, but in practice liquid sodium silicate glass can be applied on the refractories by spraying or coating with a brush. Such application methods can be used easily in combustion plants boilers.

4. Conclusions

Impregnation of fireclay refractory castable with liquid sodium silicate glass under vacuum increased the density, ultrasonic pulse velocity, cold crushing strength, modulus of elasticity and reduced porosity, compacted the microstructure and increased resistance to alkali as a result of a barrier formed (0.9-1.5mm) that prevented further penetration of alkali and stopped further disintegration of refractory castable.

The main properties of fireclay refractory castable impregnated with liquid sodium silicate glass improved because the impregnation densifies the microstructure and decreases the porosity of refractory castables by partially filling the pores and connecting capillaries, healing the microcraks and accelerates anorthite formation, which has good thermal stability properties.

The thermal shock resistance of the impregnated samples compared to the control samples can decrease about 10%, because of the improved modulus of elasticity (7-16%).

Author Contributions: "Conceptualization, J.M. and V.A.; methodology, J.M., R.B., A.K.; validation, J.M., V.A. and R.S.; formal analysis, J.M., R.B., A.K..; investigation, J.M., R.B., A.K.; resources, R.S.; data curation, J.M. and R.B.; writing—original draft preparation, J.M.; writing—review and editing, J.M., V.A., R.S; visualization, J.M., R.B.; supervision, V.A.; project administration, R.S.; funding acquisition, R.S. All authors have read and agreed to the published version of the manuscript.".

Funding: This research received no external funding.

Institutional Review Board Statement: Not applicable.

Informed Consent Statement: Not applicable.

Conflicts of Interest: The authors declare no conflict of interest.

References

1. Vares, V.; Kask, U.; Muiste, P.; Pihu, T.; Soosaar, S. Biofuel user manual, TutPress 2005, 178.
2. Rosendahl, L. Biomass combustion science, technology and engineering, Woodhead Publishing, Netherland, 2013, 40, 301.
3. European council – conclusion, Brussels, Belgium, 2014 https://www.consilium.europa.eu/media/24561/145397.pdf
4. Klinger, W.; Weber, W.; Zimmermann, H. Application concepts of shaped and unshaped refractories for combustion plants, Proceedings of UNITECR 2007, 2007, 440–443.
5. Antonovič, V. Refractory materials for biofuel boilers: Chapter 22 / V. Antonovič, J. Szczerba, J. Kerienė, R. Stonys, R. Boris//Frontiers in bioenergy and biofuels, InTech, Rijeka, Croatia, 2017, 443–464.
6. Mahapatra, M.K. Review of corrosion of refractory in gaseous environment. Int. J. Appl. Ceram. Technol 2020, 17, 606–615. https://doi.org/10.1111/ijac.13418
7. Alibasic, E.; Oldin, J.; Kannabiran, S. Design of castables and their relevance to alkali resistance applications, in proc. of the 57th Intern. Colloquium on Refractories EUROGRESS, Aachen, Germany, 2014, 67–69.
8. Taylor, J. R.; Bull, A.C. Ceramics glaze technology. Printed in Great Britain by A. Wheaton & Co. Ltd, Exeter. 1986, 276 p.
9. Parr, C.; Simonin, F.; Touzo, B.; Wohrmeyer, C.; Valdelievre, B.; Namba, A. The impact of calcium aluminate cement hydration upon the properties of refractory castables, Kerneos Aluminate Tech., 2004, 1–17.
10. Scudeller, L. A. M.; Longo, E.; Varela, J. A. Potassium Vapor Attack in Refractories of the Alumina-Silica System, J. Am. Ceram. Soc. 1990, 73(5), 1413–1416. https://doi.org/10.1111/j.1151-2916.1990.tb05214.x
11. Kerienė, J.; Boris, R.; Antonovič, V.; Stonys, R.; Škamat, J. Action of the products of biofuel combustion on the phase composition and structure of refractory material, Glass and ceramics, 2016, 72(9–10), 345–350. https://doi.org/10.1007/s10717-016-9788-9
12. Carlborg, M.; Bostrom, D.; Ohman, M.; Backman, R. Reactions between ash and ceramic lining in entrained flow gasification of wood – exposure studies and thermodynamic considerations. 21st European Biomass Conference and Exhibition 2013, 446–449.
13. Brunk, F. Silica refractories. CN Refractories, Special Issues, 2001, 5, 27–30. https://www.pd-refractories.com/files/Dokumente/Publikationen/Silica-Refractories_2001.pdf
14. Goswami, G.; Sanu, P.; Panigrahy, P. K. Estimation of thermal expansion of silica refractory based on its mineralogy, Interceram Refractories Manual, 2015, 64, 174–176. https://doi.org/10.1007/BF03401118
15. Baspinar, M.; Serhat, K. F. Optimization of the corrosion behaviour of mullite refractories against alkali vapour via ZrSiO4 addition to the binder phase, Ceramics Silikaty, 2009, 53(4), 242–249. https://www.ceramics-silikaty.cz/2009/pdf/2009_04_242.pdf
16. Vargas, F.; Restrepo, E.; Rodríguez, J. E.; Vargas, F.; Arbeláez, L.; Caballero, P.; Arias, J.; López, E.; Latorre, G.; Duarte, G. Solid-state synthesis of mullite from spent catalysts for manufacturing refractory brick coatings, Ceram. Int., 2018, 44(4), 3556–3562. https://doi.org/10.1016/j.ceramint.2017.11.044
17. Ren, B.; Shaobai, S.; Yawei, L.; Shengli, J. Correlation of pore structure and alkali vapor attack resistance of bauxite-SiC composite refractories, Ceram. Int., 2015, 41(10), 14674–14683. https://doi.org/10.1016/j.ceramint.2015.07.190
18. Ren, B.; Shaobai, S.; Yawei, L.; Yibiao X. Effects of oxidation of SiC aggregates on the microstructure and properties of bauxite-SiC composite refractories, Ceram. Int., 2015, 41 (2), 2892–2899. https://doi.org/10.1016/j.ceramint.2014.10.114
19. Butzbach, K. Hasle have a long tradition for producing highly alkali resistant refractory castables, Hasle Refractories, 2019, 125 p.
20. Zawraah, M. F. M.; Khalil, N. M. Effect of mullite formation on properties of refractory castables, Ceram. Int., 2001, 27(6), 689–694. https://doi.org/10.1016/S0272-8842(01)00021-9

21. Malaiškienė, J.; Antonovič, V.; Boris, R.; Stonys, R. Improving the physical and mechanical properties and alkali resistance of fireclay-based castables by modifying their structure with SiO2 sol, Ceramics international, 2022, 48(15), 22575–22585. https://doi.org/10.1016/j.ceramint.2022.04.278
22. Kobayashi, W. T.; Paulo, S.; Da Silva, E. L.; Carlos, S.; Paskocimas, C. A. Method for producing corrosion resistant refractories. United States Patent 2003, No.: US 6,667,074 B2.
23. Khlystov, A.; Konnov, M.; Shirokov, V. Resource and energy saving technologies of refractory linings of thermal units, MATEC Web of Conferences, 2017, 106, 1–7.
24. Lianying, Z.; Bo, P.; Jiandong, W.; Xiaofeng, Y.; Lianwei, F. Waterproof treatment method for magnesium refractory bricks, Patent, 2013, No.CN103172405.
25. Ben, D.; David, N. Refractory brick. Patent, 1970, No. US3489580.
26. Moiseevich, L.A.; Yurevich, M.T., Yarushina T.; Aleksandrovich O.M. Refractory product and method of its production, Patent No. RU2638065.
27. Fard, F. G.; Talimian, A. Improving Corrosion Behaviour of Magnesia-Chrome Refractories by Addition of Nanoparticles, Refractories World Forum, 2014, 6(2), 93–98.
28. Malaiškienė, J.; Antonovič, V.; Boris, R.; Stonys, R. Effect of the impregnation with liquid glass on the properties of refractory castable, Unified International Technical Conference on Refractories (UNITECR) 18th Biennial Worldwide Congress on Refractories, 26th-29th September 2023, Germany, Frankfurt am Main: proceedings: The carbon challenge. Steps & leaps to master the future. Höhr-Grenzhausen: European Centre for Refractories gGmbH (ECREF), ISBN 9783981581393, 2023, 834-838.
29. Antonovič, V.; Stonys, R.; Zdanevičius, P.; Mačiulaitis, R.; Boris, R.; Malaiškienė, J. Analysis of the formed protective layer inhibiting alkali corrosion in aluminosilicate refractory castables, Ceramics: Special issue: Advances in ceramics. 2022, 5(4), 1051–1065. https://doi.org/10.3390/ceramics5040075
30. Antonovich, V.; Shyukshta, M.; Pundene, I.; Stonis, R. Procedural elements in estimation of the thermal shock resistance of different types of refractory concrete based on chamotte filler, Refract. Industr. Ceram., 2011, 52(1), 70–74.
31. Niyogi, S.K.; Das, A.C. Prediction of thermal shock behaviour of castable refractories by sonic measurements, Refractories, 1994, 43(6), 453–457.
32. Csaki, S.; Lukac, F.; Húlan, T.; Veverka, J.; Knapek, M. Preparation of anorthite ceramics using SPS. Journal of the European Ceramic Society, 2021, 41(8), 4618–4624. https://doi.org/10.1016/j.jeurceramsoc.2021.03.004
33. Nishikawa, A. Technology of Monolithic Refractories; Japan by Toppan Printing Company: Tokyo Japan, 1984; 598p.
34. Malaiškienė, J.; Antonovič, V.; Boris, R.; Stonys, R. Improving the physical and mechanical properties and alkali resistance of fireclay-based castables by modifying their structure with SiO2 sol. Ceramics international, 2022, 48(15), 22575–22585. https://doi.org/10.1016/j.ceramint.2022.04.278
35. Magliano, M.V.M.; Prestes, E.; Medeiros, J.; Veiga, J.L.B.C.; Pandolfelli, V.C. Colloidal silica selection for nanobonded refractory castables. Refractories Applications and News, 2010, 15(3), 14-17.
36. Li, N.; Vainio, E.; Hupa, L.; Hupa, M.; Zabetta, E.C. Interaction of high Al_2O_3 refractories with alkaline salts containing potassium and sodium in biomass and waste combustion. Energy Fuels, 2018, 32, 12971–12980. https://doi.org/10.1021/acs.energyfuels.8b03136
37. Niu, Y.; Wang, Z.; Zhu, Y.; Zhang, X.; Tan, H.; Hui, S. Experimental evaluation of additives an K_2O-SiO_2-Al_2O_3 diagrams on high temperature silicate melt-induced slagging during biomass combustion. Fuel, 2016, 179, 52-59. https://doi.org/10.1016/j.fuel.2016.03.077
38. Ulbricht, J.; Dudczig, S.; Tomšu, F.; Palco, S. Technological measures to improve the thermal shock resistance of refractory materials, Interceram Refract. Man., 2012, 2, 103–106.
39. Szczerba, J.; Pedzicha, Z.; Nikiel, M.; Kapuscinska, D. Influence of raw materials morphology on properties of magnesia-spinel refractories. Journal of European Ceramics Society, 2007, 27, 1683–1689. https://doi.org/10.1016/j.jeurceramsoc.2006.04.145